



UNIVERSITÀ
DEGLI STUDI
FIRENZE

FLORE

Repository istituzionale dell'Università degli Studi di Firenze

Thermo-optic durability of cool roof membranes: Effect of shape stabilized phase change material inclusion on building energy

Questa è la versione Preprint (Submitted version) della seguente pubblicazione:

Original Citation:

Thermo-optic durability of cool roof membranes: Effect of shape stabilized phase change material inclusion on building energy efficiency / Fabiani C.; Piselli C.; Pisello A. L.. - In: ENERGY AND BUILDINGS. - ISSN 0378-7788. - STAMPA. - 207:(2020), pp. 109592.1-109592.11. [10.1016/j.enbuild.2019.109592]

Availability:

The webpage <https://hdl.handle.net/2158/1286093> of the repository was last updated on 2022-10-26T17:48:01Z

Published version:

DOI: 10.1016/j.enbuild.2019.109592

Terms of use:

Open Access

La pubblicazione è resa disponibile sotto le norme e i termini della licenza di deposito, secondo quanto stabilito dalla Policy per l'accesso aperto dell'Università degli Studi di Firenze (<https://www.sba.unifi.it/upload/policy-oa-2016-1.pdf>)

Publisher copyright claim:

La data sopra indicata si riferisce all'ultimo aggiornamento della scheda del Repository FloRe - The above-mentioned date refers to the last update of the record in the Institutional Repository FloRe

(Article begins on next page)

Thermo-optic durability of cool roof membranes: effect of shape stabilized phase change material inclusion on building energy efficiency

C. Fabiani¹, C. Piselli^{1,2}, A.L. Pisello^{1,2}

¹*CIRIAF - Interuniversity Research Centre, University of Perugia, Italy. Via G. Duranti 63 06125 Perugia (Italy)*

²*Department of Engineering University of Perugia, Italy. Via G. Duranti 93 06125 Perugia (Italy)*

Abstract

Cool roofs represent an acknowledged passive cooling technique aimed at reducing the amount of solar radiation absorbed by buildings and producing indoor overheating, particularly, in summer conditions. Cool roofs owe their unique behavior to improved thermo-optic performances which, however, have been shown to deteriorate when exposed to intense atmospheric weathering. In this context, the authors produced a shape stabilized composite with improved heat storage performance, by adding 15, 25 or 35 weight percentage of non-encapsulated phase change materials (PCMs) to the original blend of a liquid waterproof-polyurethane-based cool membrane. The behavior of such composite material, when exposed to accelerated temperature, humidity, and UV radiation cycles by means of standardized long-term weathering tests (QUV test), is investigated. The final aim of the study is to clarify if the PCM inclusion could help the membrane to better behave during the course of the time, because of thermal stress reduction. In order to do so, controlled atmospheric forcing and surface temperature continuous monitoring are used to investigate the degradation of the membrane produced by the imposed weathering stress. Results show that the introduction of 25% PCM in weight optimizes the superficial finishing characteristics of the prototype, allowing to maintain a more stable thermo-optic behavior, reducing both the thermal-induced degradation and the leakage phenomenon.

Keywords: Cool roofs, Phase change material, Shape stabilize material, Weathering analysis, QUV, Thermal energy storage in buildings,

1. Introduction

In the last decades, the awareness about the energy and environmental role of the built environment to meet the European 2020 targets [1] has attracted the focus of researchers [2]. Several solutions for building energy efficiency were developed and acknowledged [3]. In particular, the energy consumption for cooling has been gaining attention due to the raising use of active cooling systems for contrasting the overheating associated to climate change and urban development [4]. Indeed, a worldwide increase of cooling degree days was demonstrated [5]. Therefore, the introduction of passive cooling techniques, capable of reducing summer overheating phenomenon, could play a significant role in the achievement of the global energy consumption reduction targets [6]. Such mitigation and adaptation strategies are effective both at the building scale and at the district or city scale for the restoration of natural passive cooling [7]. Among passive cooling strategies, cool materials are capable to induce a negative radiation forcing by reflecting the shortwave radiation back to space [8]. Therefore, they allow to counteract the global warming, cooling down urban heat islands [9], and reduce the cooling energy use and the associated demand for power, consumption of fuel, greenhouse gas emissions, and air pollutants in buildings [10]. In details, direct energy savings and emission reductions can be achieved thanks to the reduction of envelope solar heat gains [11, 10], while indirect savings from reducing the air temperature difference across the building envelope [12, 13]. In particular, cool roofs were demonstrated to save annual energy consumption in all buildings needing for cooling, with negligible heating penalties in winter, precluding the need to install any air conditioning system under certain boundary conditions [14]. For instance, Hernández-Pérez et al. [15] showed a daily heat gain reduction through the roof up to about 80% thanks to a cool coating with respect to a conventional roof. Moreover, bismuth titanate (BTO) was demonstrated to be a potential cool pigment with even higher reflectance property than the conventional TiO_2 pigment, for energy saving applications [16].

On the other hand, the proper inclusion of phase change materials (PCMs) in the building envelope as passive thermal energy storage application enhances its energy storage capability [17, 18]. Therefore, indoor thermal

35 conditions are improved by balancing the environmental temperature and
 36 dampening its fluctuation [19]. In this view, one of the main technical is-
 37 sues is how to effectively integrate such material within the building envelope
 38 [20], while preventing leakage and volatilization and ensuring material con-
 39 servation [21]. To solve this problem, shape-stabilized PCMs is one of the
 40 methodologies currently being used for encapsulation [22]. It consists on the
 41 fixation of the phase change material within a matrix, by blending it with
 42 a suitable polymer, which results in the suppression of leakage in the liquid
 43 phase [23]. Different shape-stabilization procedures were tested for various
 44 applications, e.g. a form-stable composite using diatomite (a type of natural
 45 non-metallic mineral material) as supporting material [24]. This procedure
 46 can be effectively implemented also by coupling cool roof materials and PCMs
 47 [25, 26]. The combination of high reflectivity and phase change materials
 48 for the building envelope has been narrowly studied, showing potentialities
 49 both for building energy efficiency [27] and urban heat island phenomenon
 50 mitigation [28]. Lu et al. [29], for example, developed and experimentally
 51 monitored a novel roof coupling a PCM-eutectic mixture layer (homogeneous
 52 mixture of two materials) and a cool roof coating, which showed a smoother
 53 temperature fluctuation and higher thermal insulation with respect to the
 54 simple cool roof. Focusing on cool roof coating thermal stress reduction,
 55 Saffari et al. [30] defined the optimum PCM melting temperature to reduce
 56 cool roof membrane thermal stress, while minimizing building annual energy
 57 needs in different climate zones worldwide.

58 Nevertheless, the demonstrated benefits achievable by such strategies can
 59 be compromised during their life span due to material aging associated to
 60 weathering [31], soiling [32, 33, 34], and biological growth [35]. Although
 61 albedo changes induced by weathering, they can be reduced by an accurate
 62 maintenance procedure, e.g. wiping, rinsing, and washing [36]. However, the
 63 same technique is not as effective in reducing natural weathering alterations.
 64 Additionally, although cool materials aging seems not to represent a barrier
 65 for their energy efficiency, performance loss over time must be understood
 66 [37]. Several studies quantified the effect of natural exposure on solar re-
 67 flectance [38, 39]. For instance, Ferrari et al. [40] analyzed the influence of
 68 natural aging on the solar reflectance of clay roof tiles.

69 De Masi et al. [41] found, through in-field test, that the solar reflectance
 70 of an acrylic white paint for cool roof applications can decrease from 0.67 to
 71 0.48 after 1 year of exposure to the outdoor environment. Similarly, Aoyama
 72 et al. [42] demonstrated the increased durability due to the self-cleaning

73 capability of a high-reflectance coating subjected to outdoor exposure test.
 74 However, such in-field tests require long-time exposure to provide interesting
 75 results. Therefore, accelerated weathering techniques, such as QUV test [43],
 76 have been developed to provide a shorter test period. In such a test, materi-
 77 als are alternately exposed to temperature cycling, UVA radiation, and water
 78 condensation to accelerate natural environments with higher stress, without
 79 changing the failure mechanism [44]. The QUV test is typically used to assess
 80 materials mechanical failure, but it can also be used to predict the variation
 81 in the thermo-optical performance of materials [45]. Since no unequivocal
 82 correspondence can be established between accelerated and real weathering
 83 due to the large variability on the possible local boundary conditions, real
 84 exposure is generally preferred to the accelerated one. However, QUV anal-
 85 ysis can produce acceptable information in terms of comparative behavior of
 86 the investigated products with a lower effort in terms of experimental time.
 87 Santunione et al. [46], for instance, assessed the capability of an acceler-
 88 ated test method to investigate the consequences of biological aggression on
 89 coating materials.

90 To verify the durability of materials thermal-energy performance before
 91 and after the aging process, dynamic analysis can be carried out in controlled
 92 conditions [47]. This procedure allows to investigate the dynamic behavior of
 93 building materials and components with a better reliability than real building
 94 applications, frequently affected by extra-variables such as occupancy [48].
 95 Ricciu et al. [49] used this methodology for the thermal characterization
 96 of different insulating materials, compared to more traditional procedures,
 97 while D'Alessandro et al. used it to characterize the thermal buffer capabil-
 98 ity of innovative PCM-doped concretes for structural applications [50]. In
 99 order to assess the performance of PCM-doped cool roof tiles, Chung and
 100 Park [51] simulated summer weather conditions in an artificial environment.
 101 The measurements enabled to demonstrate the capability of PCM to further
 102 reduce roof external surface temperature, while improving indoor thermal
 103 comfort throughout the year.

104 Based on the above, a novel composite material combining polyurethane
 105 liquid waterproof-polyurethane-based cool membrane with different percent-
 106 ages of non-capsulated PCMs was developed for roof applications [52, 26].
 107 When combining PCMs and cool roofs, exposure to sun, rain, and wind are
 108 critical factors to be taken into account, since they significantly influence the
 109 thermo-mechanical response of the membrane, determining the detrimen-
 110 tal leakage phenomenon. Therefore, the composite material was exposed to

111 accelerated weathering long-term tests (QUV test), to assess the cool mem-
112 brane vulnerability to real environmental forcing. In a previous paper [45],
113 the same authors evaluated the influence of PCMs inclusion, on the durabil-
114 ity of the cool membrane mostly in terms of thermal properties, morphology,
115 and mechanical response. Following up from these studies, the purpose of
116 this work is to further analyze the capability of PCMs to preserve the cool
117 membrane thermal-energy performance over time, due to thermal stress re-
118 duction. In detail, thermo-energy dynamic-analysis of the aged composite
119 material was developed in a controlled environmental chamber to assess the
120 role of the PCM in reducing the PCM-doped cool roof surface temperature
121 [48, 50].

122 2. Materials and sample preparation

123 In this work, the long-term durability of a polyurethane-based-white-
124 liquid membrane for non-sloped roof applications developed by the authors
125 in a previous research work [52, 26] is experimentally investigated. The afore-
126 mentioned membrane is optimized by using titanium dioxide (TiO_2 , in the
127 form of rutile) and hollow ceramic micro-spheres, to increase its passive cool-
128 ing potential. Additionally, an organic paraffin with a melting point of 25
129 °C and a heat storage capacity of $148 \text{ kJ}\cdot\text{kg}^{-1}$ is also introduced within the
130 mixture, with the aim of preserving better spectral reflectance in the near
131 infrared region of the solar spectrum. Additionally, the smallest possible al-
132 teration during the course of accelerated weathering (QUV) tests together
133 with the maintaining of the required flexibility and superficial finishing char-
134 acteristics, was also sought.

135
136 The prototype membranes were produced by simply mixing the solid-state
137 non-encapsulated paraffin within the membrane tank with liquid polyurethane,
138 while keeping an ambient temperature of 20 °C to prevent the PCM from
139 melting during this phase. In the previous works, three different specimens
140 were produced, i.e. a reference “pure-cool” membrane with no additives
141 (noOPT), a cool membrane with “optimized-cool” surface (OPT) and three
142 cool membranes with 15%, 25%, and 35% in weight of PCM added to the
143 original mix design with titanium dioxide and the micro-spheres, i.e. 15PCM,
144 25PCM and 35PCM, respectively (see Figure 1).

145

146 Here, only the optimized-cool and the three PCM-doped membranes
 147 were selected to perform a durability investigation of the prototypes against
 148 temperature and radiation-induced mechanical stresses. In particular, four
 149 square samples with the dimension of 10 cm×10 cm were collected for every
 150 considered membrane, and exposed to different accelerated weathering times,
 151 i.e. 0, 15, 30 and 60 days.

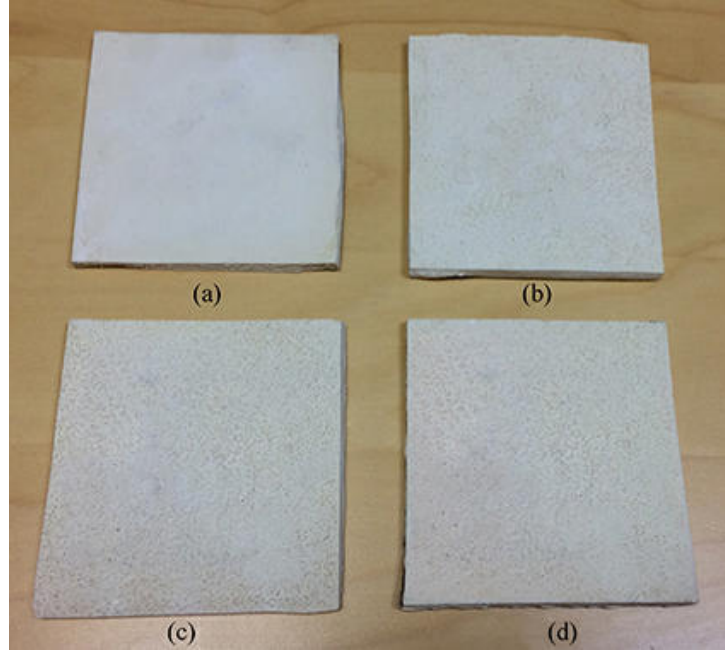


Figure 1: Investigated polyurethane membranes: (a) OPT, (b) 15PCM, (c) 25PCM, and (d) 35PCM, before the accelerated weathering procedure.

152 3. Experimental methodology

153 As reported in Figure 2, the research procedure consisted of the following
 154 main steps:

- 155 - development of the proposed cool roof solution through the integration
 156 of an organic PCM, i.e. paraffin-based material, into the polyurethane-
 157 based cool membrane in different percentages [52, 26];
- 158 - accelerated weathering procedure of the different membranes according
 159 to ASTM D 4329-99 (Standard Practice for Fluorescent Ultraviolet

- (UV) Lamp Apparatus Exposure of Plastics) [53] and ASTM G154 - 06 (Standard Practice for Operating Fluorescent Light Apparatus for UV Exposure of Nonmetallic Materials) [54];
- surface characterization of the membranes in terms of spectral near normal-hemispherical reflectance according to ASTM E903-12 (Standard Test Method for Solar Absorptance, Reflectance, and Transmittance of Materials Using Integrating Spheres) [55];
 - thermal characterization of the membranes at different aging times, i.e. non-aged, 15, 30, and 60 days of aging using the sol-air temperature ($T_{\text{Sol-air}}$);
 - thermal characterization of the non-aged membranes using a halogen UV-lamp and comparison with the profiles from the sol-air temperature ($T_{\text{Sol-air}}$) analysis.



Figure 2: Schematic representation of the main steps carried out in this work

3.1. Accelerated weathering test

The accelerated aging test was carried out by using a QUV machine (QUV Accelerated Weathering Tests, Q-Lab) and according to the international standards ASTM D 4329-99 [53], linked to the operative procedure described in the ASTM G154-06 [54]. The samples were repeatedly exposed to the following forcing conditions:

- 179 - 8 hours of UVA radiation (340 nm, energy of $0.77 \text{ W}\cdot\text{m}^{-2}$) at 50°C ;
- 180 - 2 hours in humid condition (100 RH%) at 40°C ;
- 181 - 2 hours in humid condition (100 RH%) at 20°C .

182 According to ASTM G154-06 standard, any exposure conditions, pro-
183 vided that they are fully described, may be used in the investigation pro-
184 cedure. All this considered, the conditioning cycle used in this work was
185 specifically designed by the authors in order to reproduce environmental con-
186 ditions that could be representative of the peak temperature and humidity
187 conditions characterizing climate areas where cool roof solutions are typically
188 recommended and applied as passive cooling systems for building energy ef-
189 ficiency.

190
191 The effect of the accelerated weathering test on the different samples of
192 cool membranes was evaluated after 15, 30, and 60 days of exposure, based
193 on the common practice derived from the two reference ASTM standards
194 [53, 54]. More in detail, three samples per type were exposed to the test.
195 The first series of samples, one for each type (OPT, 15PCM, 25PCM, and
196 35PCM), was extracted out of the machine after 15 days, the second series
197 was extracted after 30 days, and the last series was extracted after 60 days.

198 *3.2. Spectral near normal-hemispherical reflectance*

199 The in-lab optical characterization of all the samples was carried out by
200 means of a Solid Spec 3700 UV–vis–NIR spectrophotometer equipped with a
201 60 mm integrating sphere coated with barium sulfate, in the range 300–2500
202 nm according to the ASTM E903-12 [55] standard method. Five different
203 spectral near normal-hemispherical reflectance measurements were taken for
204 each of the 16 samples, by measuring different geometrical positions on the
205 membranes, in order to produce a reliable statistic representation of the optic
206 behavior of the innovative coatings.

207 *3.3. Thermal monitoring in real dynamic conditions*

208 The thermal characterization of the membranes was carried in two differ-
209 ent stages. First, each membrane was exposed to a hygro-thermal condition-
210 ing cycle using the sol-air temperature. Secondly, the non-aged samples were
211 exposed to an additional hygro-thermal forcing procedure, making use of a

212 solar simulator to reproduce the incoming radiative flux. The former proce-
 213 dure was aimed at evaluating the differential response of the membranes after
 214 different aging times; the latter, at comparing the thermal profiles produced
 215 using the sol-air temperature (defined in more details in the following) with
 216 the ones registered using the solar simulator.

217 Both analyses were carried out using an ATT DM340SR climatic cham-
 218 ber equipped with a test compartment (601 mm×810mm×694 mm) where
 219 it is possible to obtain a temperature- and humidity-controlled environment
 220 in the range $-40\text{--}180\text{ }^{\circ}\text{C} \pm 0.5\text{ }^{\circ}\text{C}$ and $10\text{--}98\% \pm 3\%$ of RH [56]. The chamber
 221 is also equipped with a solar simulator, i.e. a halogen lamp operating in
 222 the power range 600 to 1200 W (solar spectrum shown in Figure 3), and 12
 223 PT-100 temperature sensors. The environmental chamber ensured the high
 224 stability of the tests, compared to field experiments, and the repeat ability
 225 of the same experiments for bench-marking purposes.

226

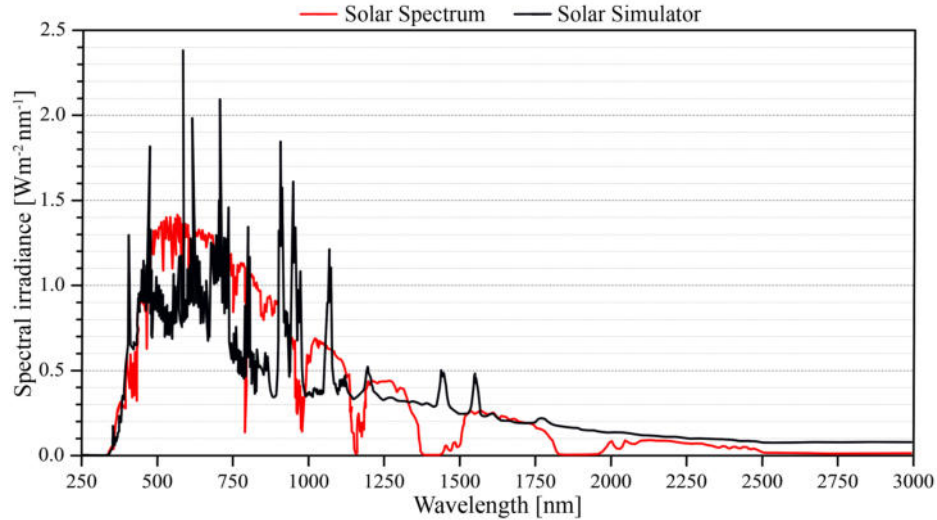


Figure 3: Spectrum of the solar simulator (halogen lamp) compared to the AM 1.5 direct solar spectrum from ASTM G173-03(2012) (Standard Tables for Reference Solar Spectral Irradiances: Direct Normal and Hemispherical on 37° Tilted Surface) [57]).

227 During the experimental campaign, each type of membrane was housed
 228 within the controlled environment of the climatic chamber, and exposed to
 229 specifically designed environmental cycles. More in detail, real meteorological
 230 data from a weather station located on the rooftop of a University building

located in central Italy (Perugia) were used to investigate the effect of the selected phase change materials on the long-term durability of the advanced cool roof membranes. In particular, weather data from a typical hot summer day, i.e. 2017-07-26, were selected to be reproduced within the simulated environment of the climatic chamber (see Figure 5).

During the experimental campaign, the membranes were placed in a specifically designed polyurethane (PUR) sample holder, assembled in order to completely protect and insulate five surfaces out of six, i.e. the four sides and the bottom surface, while leaving the upper one exposed to the controlled environment of the chamber (see Figure 4).

10 T-type thermocouples were shielded with an aluminum tape and used to monitor the thermal behavior of each sample. In particular, five T-type sensors were attached at the upper surface of the membranes, while the remaining five probes were placed at the bottom surface, as shown in Figure 4. The thermocouples were connected to a data acquisition system model cDAQ-9184 equipped with two NI 9213 Spring slots from National Instruments, and programmed in order to read the sensors every 30 seconds. In this way, it was possible to (i) accurately register the surface thermal profile of the roof membranes and (ii) identify the effect of the PCMs throughout the thickness of the samples during the overall extent of the monitoring process.

3.3.1. Sol-air temperature-based cycles

In the first stage of the thermal analysis, each membrane was exposed to a specifically designed, sol-air temperature-based forcing cycle (Tsol cycle), reproducing the local boundary conditions between 6:00 AM and 9:00 PM Local Standard Time (LST).

The Tsol cycle, makes use of the sol-air temperature ($T_{\text{Sol-air}}$) to combine temperature and radiative contributions in one single temperature forcing parameter, to be used in combination with the relative humidity profile.

In this case, a broader time interval (between 5:00 AM and 8:00 PM (LST)), was selected. The sol-air temperature for the horizontal roof stratigraphy exposed to the selected weather conditions was computed according to Equation 1 [58]:

$$T_{\text{Sol-air}} = T_{\text{air}} + \alpha I_g R_{\text{se}} - \Delta Q_{\text{ir}} R_{\text{se}} \quad (1)$$

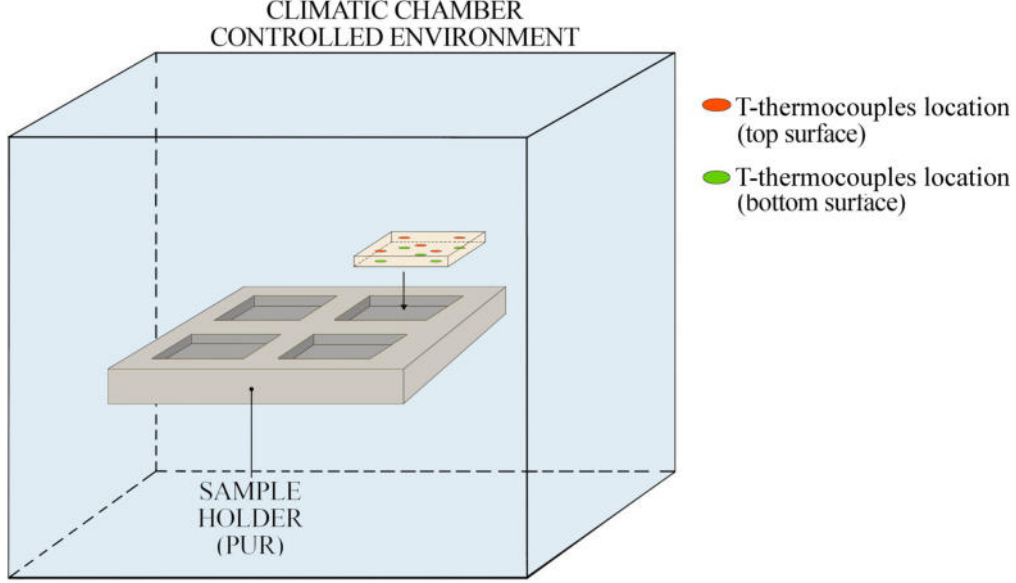


Figure 4: Schematic representation of the experimental setup.

where T_{air} is the outdoor air temperature from the weather file ($^{\circ}\text{C}$); α is the solar absorptance of the specific membranes; I_g is the global solar radiation from the weather file ($\text{W}\cdot\text{m}^{-2}$); R_{se} is the external surface resistance ($\text{m}^2\cdot(\text{K}\cdot\text{W})^{-1}$); and ΔQ_{ir} is the correction to infrared radiation transfer between surface and environment if sky temperature is different from T_{air} , ($\text{W}\cdot\text{m}^{-2}$).

The term R_{se} Equation 1, was set to $0.04 \text{ (m}^2\cdot\text{K}^{-1}\cdot\text{W}^{-1}\text{)}$, in accordance to the recommendations of ISO 6946:2017 (Building components and building elements – Thermal resistance and thermal transmittance – Calculation methods) [59]. As for the infrared radiation transfer correction, since the roof membrane represents a upward-facing surface in real applications, $\Delta Q_{\text{ir}}R_{\text{se}}$ was imposed to its maximum value, i.e. $3.9 \text{ }^{\circ}\text{C}$ [60].

Given that the sol-air temperature depends on solar absorptance, which differs by material, each membrane was separately analyzed and exposed to a unique temperature profile based on its solar absorptance. All the membranes were assumed to be opaque surfaces, therefore, the specific solar absorptance of each surface was calculated as $\alpha = 1 - \rho$, making use of the reflectance

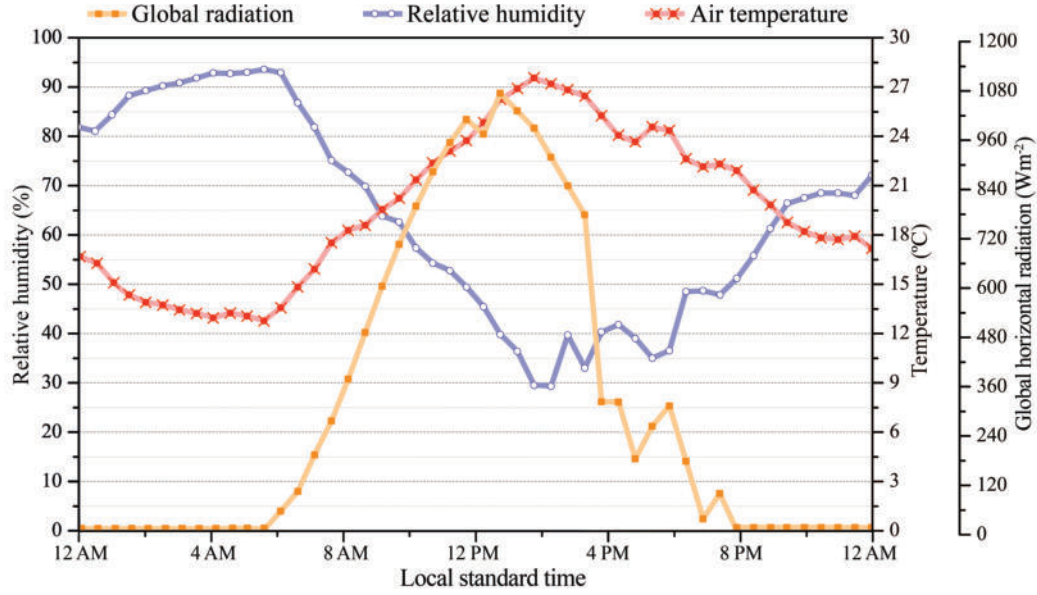


Figure 5: Relative humidity, air temperature, and global radiation (in the range 300 – 2800 nm) values registered by the weather station at Perugia University on July 26, 2017.

values presented in Section 4.1.

3.3.2. Radiation-based cycles

At a later stage, the non-aged membranes were exposed to an additional environmental cycle (the air temperature-radiation based – TaRAD – cycle), which was designed to exactly reproduce the local climatic conditions in terms of outdoor air temperature, relative humidity, and global radiation flux on the horizontal surface from 7:30 AM to 5:30 PM (LST). This specific time range was selected due to technical limitations: the solar simulator only allows to reproduce radiative fluxes above $250 \text{ W}\cdot\text{m}^{-2}$.

In contrast to the sol-air temperature-based thermal analysis, the investigation procedure carried out using air temperature and radiative flux as two separate boundary conditions allows to simultaneously analyze the thermal behavior of each type of membrane. In this case the surface interaction between the incoming radiation and the material is a real physical phenomenon occurring during the simulation. Therefore, every membrane behaves in a different way, based on its own thermo-optic properties, although exposed to the same conditioning cycle.

300

301 All this considered, using solar simulators could significantly reduce ex-
 302 perimental time. However, solar simulator are often associated to non-
 303 negligible deviations in terms of short-wave radiation accuracy, and lack of
 304 long-wave radiative exchange with the sky. In this view, the main purpose of
 305 this analysis is to compare the thermal profiles produced using sol-air tem-
 306 peratures with the ones registered using the solar simulator and evaluate the
 307 actual deviation between these conditioning techniques.

308 4. Results and discussions

309 4.1. Thermo-optic performance of the roof membranes

310 Results from the solar reflectance measurements as a function of the aging
 311 procedure are plotted in Figure 6. As can be seen, at time zero, the non-aged
 312 optimized membrane (OPT sample) presents the highest solar reflectance.
 313 Despite this, as demonstrated in a previous contribution from the same au-
 314 thors [26], the introduction of the PCMs does not result in chemical variations
 315 of the original polyurethane-based substrate. On the contrary, the two com-
 316 ponents maintain their properties and coexist in a stable form, preserving
 317 and globally combining their unique behavior. As a consequence, the exter-
 318 nal finishing of the membrane is really constituted by the only polyurethane
 319 matrix, at least, until the PCM finally leaks out of it reaching the surface.
 320 The introduction of the latent doping agent, however, increases the com-
 321 posite surface roughness, due to the presence of PCM agglomerations right
 322 beneath the surface.

323 As a consequence, larger shadows are produced and lower reflectances are
 324 obtained with increasing PCM percentages [61]. Said reduction is particu-
 325 larly large in the case of the 35PCM sample, which reaches a reflectance of
 326 0.51, before aging.

327

328 By focusing on the long-term performance of the investigated membranes,
 329 and assuming a good correlation between accelerated weathering and natural
 330 exposition effect, a different resilience capability can be observed. The QUV
 331 aging test seriously affects the optimized membrane, which significantly re-
 332 duces its reflectance with increasing weathering times (according to a quite
 333 reasonable linear trend). As for the 15PCM sample, namely the one with the
 334 minimum PCM addition, Figure 6 shows a much less stable trend, character-
 335 ized by an abrupt reflectance decrease after 15 days of aging, while after 30

and 60 days, similar performance compared to the pure membrane are found. Globally, the introduction of the PCM reduces the slope of the linear fitting curve connecting the reflectance measurements at different aging times. This brings the 15PCM sample to obtain a comparable reflectance with respect to the optimized membrane after 60 days aging.

Concerning the 25% PCM-doped solution, this particular PCM concentration shows the most promising long-term performance. The slope of the 25PCM fitting line, indeed, tends to zero in this case.

As for the 35% PCM-doped solution, the highest reflectance reduction is observed in the long-term weathering. As shown in Figure 6, the 35PCM sample solar reflection capability is initially increased, and only finally drops to 0.47 (after 60 days aging).

Furthermore, it should be stressed that both the 25PCM and the 35PCM sample experience an initial reflectance increase. This is probably caused by a positive superficial smoothing, produced by the QUV forcing cycles that reduces the drop shadows effect.

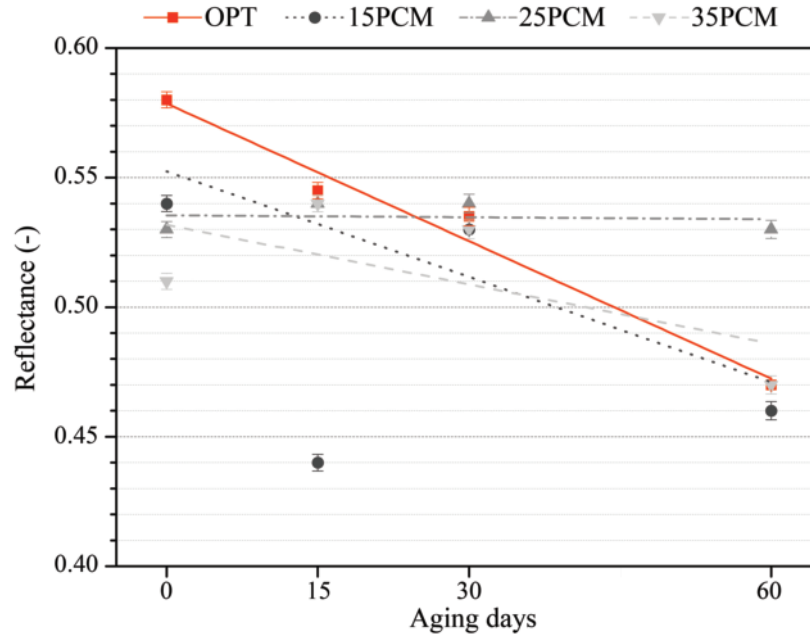


Figure 6: Total solar reflectance for the investigated polyurethane membranes, i.e. OPT-CM, 15PCM-CM, 25PCM-CM, and 35PCM-CM, before and after the accelerated weathering procedure.

Based on the above, we can state that each membrane is differently affected by the QUV test. Figure 7 shows the typical forcing profiles for a single aging day. As can be seen, during the weathering procedure each sample experiences abrupt variations in terms of temperature, relative humidity, and UVA radiation. Such variations produce intense temperature gradients and, consequently, the development of non-negligible stresses and strains in the polyurethane substrate, resulting in a complex micro-cracking pattern that globally concurs to reduce the reflectance of the OPT sample.

The introduction of PCMs, being capable to store part of the heat in the latent form, is expected to reduce such temperature gradients and the albedo degradation with it. However, only the 25PCM sample maintains a higher reflectance throughout the aging. This suggests that PCM concentrations around 15% and 35% do not allow the latent additive to fulfill its buffer task. In particular, it seems that lower PCM concentrations do not guarantee enough energy density to overcome the detrimental mechanical deterioration of the substrate, which consequently experiences a similar thermally-driven micro-cracking process. Therefore, as experienced by a direct visual and tactile inspection, the liquid PCM leaks out of the membrane already after 15 days aging, reducing its surface reflectance.

Higher concentrations, on the other hand, initially allow to produce the expected buffering effect. However, on the long-term the 35PCM sample experiences a similar drop in reflectance to the one found in the 15PCM after 15 days. This, together with the results from the visual and tactile inspection, suggests that leakage eventually occurs also in this case, but only at a later stage and most probably because of the higher PCM concentrations in the composite.

As a consequence, in the long-term, despite the occurrence of different deterioration mechanisms, both the 15PCM and the 35PCM, mostly behave as the OPT membrane.

4.2. Effect of phase change materials on the surface temperature of the aged cool roof membranes

Figure 8 shows the comparison among different surface temperature profiles monitored during the imposed T_{sol} cycles for each kind of membrane and weathering time. In particular, profiles with the same QUV exposure time are grouped and plotted on the same panel, allowing us to compare

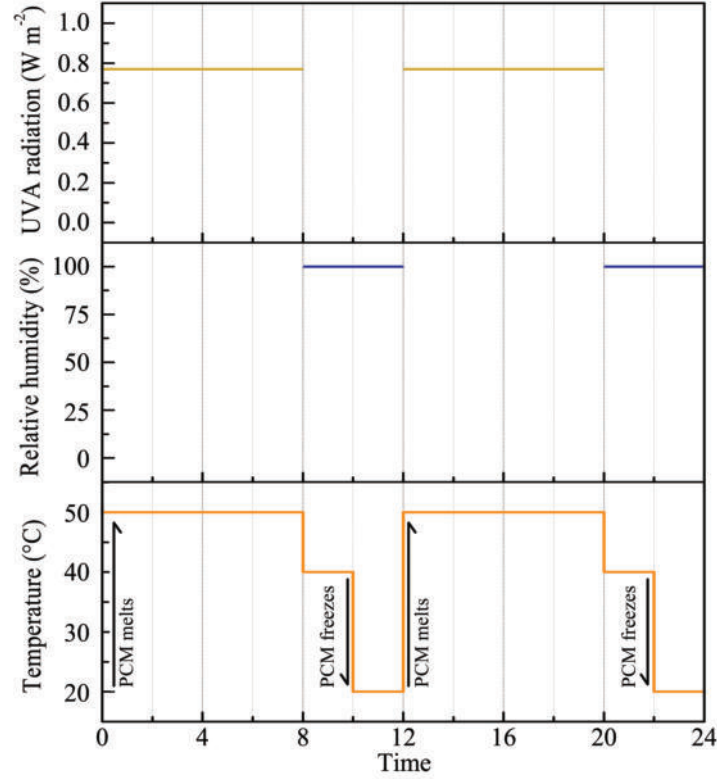


Figure 7: Forcing profiles for a typical QUV aging day.

the differential thermal response of the membranes when exposed to similar weathering conditions.

As expected, at time zero the TiO_2 -optimized membrane with no PCM addition produces the lowest surface temperature profile, exceeding 40°C only in the central part of the day (between 11:45 AM and 1:27 PM (LST), as shown in Figure 10 and Table 1). Concerning the three considered PCM-doped solutions, according to the previously described solar reflectances, an increased temperature trend is produced when increasing the weight percentage of the latent additive in the roofing membrane. However, no significant difference can be seen between the 25 and the 35% PCM solution. After 15 days of accelerated weathering, the reference optimized membrane with no PCM suffers by a non-negligible temperature increase, featuring a wider temperature bell with a peak value of 45.3°C versus the 41.2°C registered before the aging process. Additionally, Figure 10 shows that the 15-days-aged op-

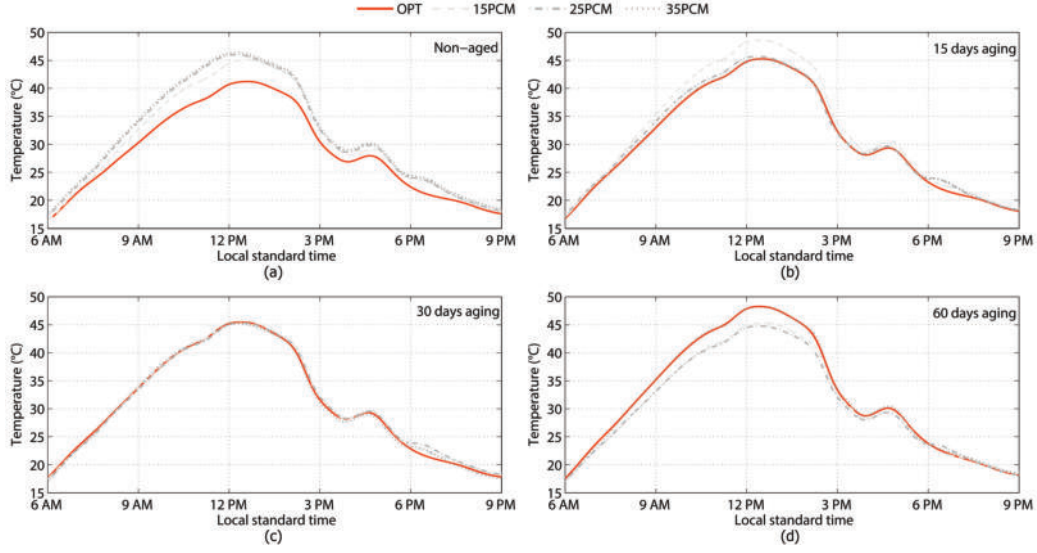


Figure 8: Comparison among the different superficial temperature profiles from the Tsol cycles considering the same accelerated weathering time, i.e. (a) 0 days, (b) 15 days, (c) 30 days, (d) 60 days.

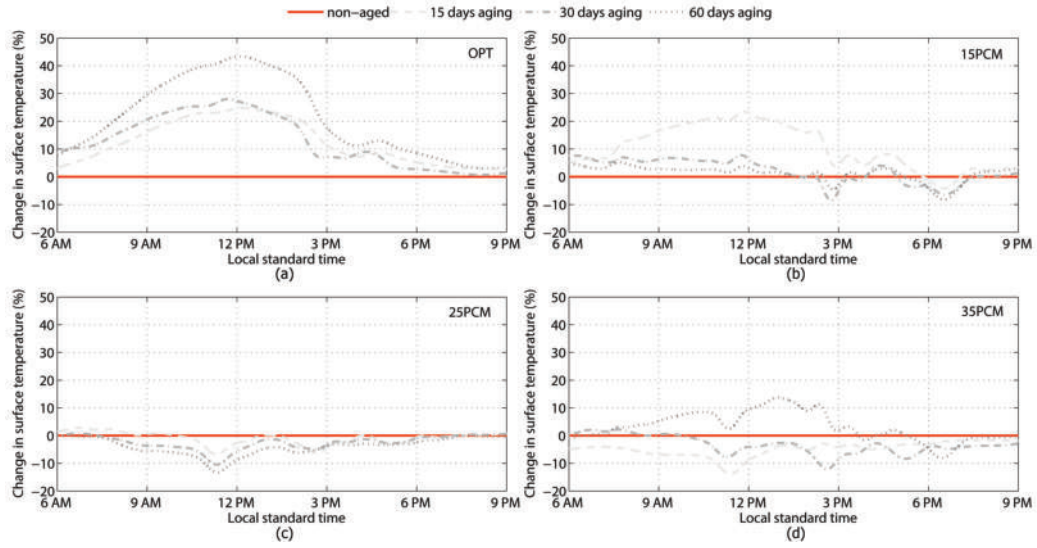


Figure 9: Change in surface temperature of the considered membranes, i.e. (a) OPT, (b) 15PCM, (c) 25PCM, (d) 35PCM, when exposed to 15, 30, and 60 days of accelerated weathering procedure with respect to the maximum air temperature difference registered in the selected day $(T_{\text{aged}} - T_{\text{non-aged}}) / (T_{\text{air,max}} - T_{\text{air,min}})$.

Table 1: Peak temperature value and local standard time at which it was registered in each of the selected membranes, considering different aging periods (0, 15, 30, and 60 days).

Aging days	opt		15PCM		25PCM		35PCM	
	LST	T	LST	T	LST	T	LST	T
	[hh:mm]	[°C]	[hh:mm]	[°C]	[hh:mm]	[°C]	[hh:mm]	[°C]
0	12:52	41.2	12:27	45.1	12:11	46.0	12:11	46.4
15	12:24	45.3	12:31	48.6	12:13	45.7	12:15	45.2
30	12:38	45.5	12:26	45.7	12:24	45.7	12:10	45.7
60	12:25	48.3	12:31	45.3	12:23	45.3	12:28	48.1

timized membrane maintains its temperature above 40 °C for about 3 hours and 52 minutes, while the original material only exceeded this limit for 1 hour and 45 minutes. Such an abrupt variation of the optimized membrane performance, allows both the 25PCM and the 35PCM sample to obtain similar thermal performance compared to the OPT sample after 15-days-aging. The 15PCM sample, on the other hand, similarly to the optimized membrane experiences a significant surface temperature increase producing a temperature peak of 48.6 °C.

After 30 days, all the membranes seem to behave in a similar way and are associated to an almost indistinguishable trend. Finally, after 60-days-aging, the reference membrane with no PCM and the 35PCM solution show the worst thermal response reaching more than 48 °C in the central part of the day.

Based on the aforementioned results, we can state that the addition of PCM to the original polyurethane mixture affects the stability of the membranes thermo-optical performance in time. In order to more carefully investigate this phenomenon, we focused our attention on the percentage change in surface temperature, defined as the difference between the surface temperature of the aged sample (T_{aged}) and the corresponding non-aged one ($T_{\text{non-aged}}$), over the maximum air temperature difference registered in the selected day ($T_{\text{air,max}} - T_{\text{air,min}}$). Figure 9 depicts said variation, grouping the membranes in four different panels (one for each type of membrane), i.e. OPT, 15PCM, 25PCM, and 35PCM.

Results demonstrate that the optimized membrane with no PCM addition is associated to the highest variations. In more detail, after 15 days of aging, an average variation by 10.2% is found, while average differences by about

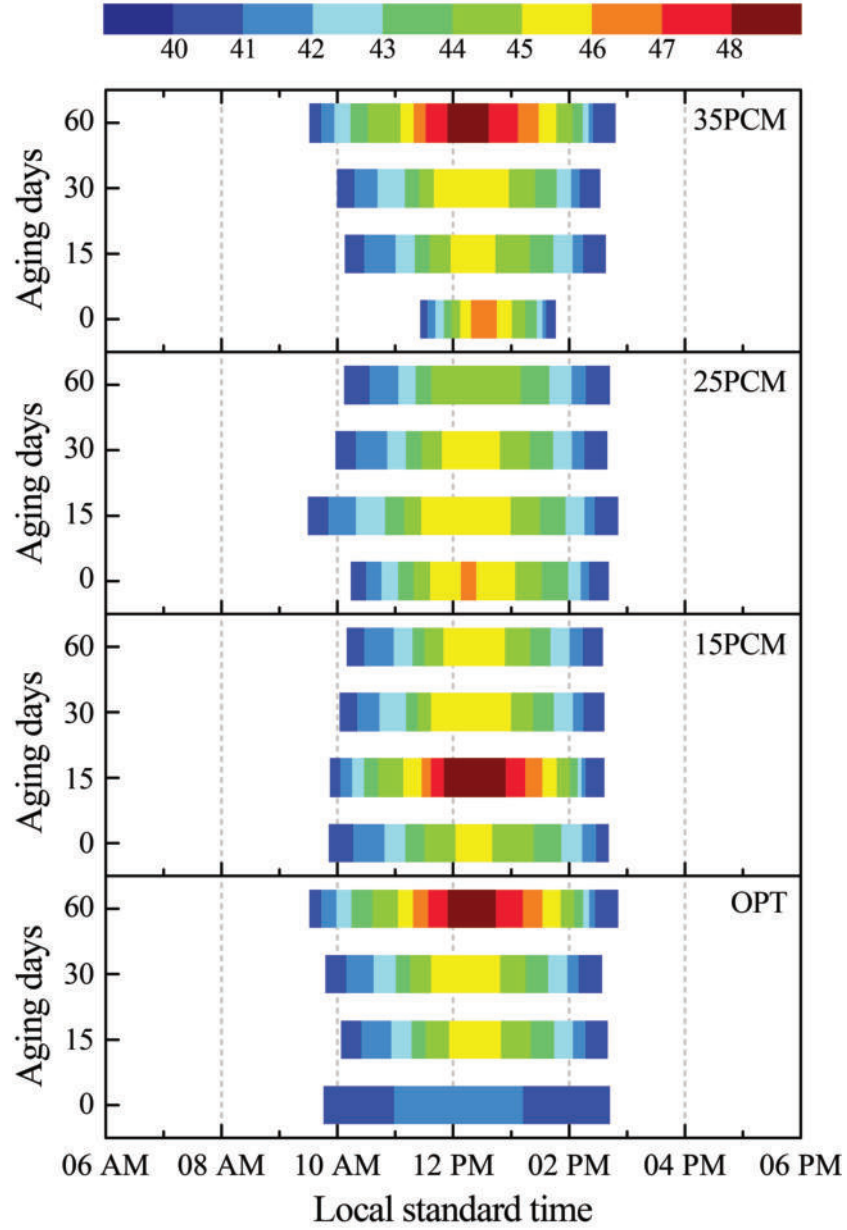


Figure 10: Time spent at temperatures above 40 °C for the investigated polyurethane membranes, i.e. (a) OPT-CM, (b) 15PCM-CM, (c) 25PCM-CM, and (d) 35PCM-CM, before the accelerated weathering procedure.

430 10.9 and 17.6% characterize the membrane after 30 and 60 days of weather-
 431 ing, respectively. Globally, the weathering process causes an abrupt decrease
 432 in the thermo-optic performance of the OPT membrane, which seemed to
 433 stabilize in the medium distance and eventually decrease again after 60 days
 434 of aging.

435
 436 Concerning the PCM-doped membranes, all of them maintain a more
 437 stable profile in time. However some variations can be detected among the
 438 different types considered in this work. In particular, the use of 25%-in-
 439 weight of PCM in the selected waterproof application seems to guarantee
 440 an acceptable trade-off between reduced deterioration due to thermal expan-
 441 sion and leakage-induced soiling upon weathering. The 25PCM is, indeed,
 442 the only application that allows to obtain a negative average temperature
 443 change in all three aging conditions (-0.63, -1.99, and -3.11% after 15, 30,
 444 and 60 days, respectively). This particular result suggests that the addition
 445 of the selected amount of PCM could represent a further optimization of the
 446 innovative cool roof membrane, aimed at improving its long-term durability
 447 performance.

448 *4.3. Comparison between sol-air temperature and radiation-based forcing*

449 Figure 10 shows the comparison among the surface temperature profiles
 450 of the four considered membranes exposed to the TaRAD and the Tsol cy-
 451 cles. As can be seen, the dark-grey-dashed profile, depicting the surface
 452 temperature generated by the radiation-based temperature forcing, very well
 453 reproduces the shape of the solid red-line trend, representing the thermal
 454 behavior of the same membrane exposed to the sol-air temperature-based
 455 forcing cycle. However, every graph in Figure 10 shows an average deviation
 456 of about 2 °C between the profile produced by the radiation-based temper-
 457 ature forcing (associated to higher temperatures) and the one from the Tsol
 458 cycle (the one that uses the sol air temperature simplification). Said differ-
 459 ence exceeds the expected experimental error derived from the combination
 460 of the acquisition and the environmental forcing system of about 1 °C, and
 461 it is probably due to an underestimation of the long-wave radiative exchange
 462 with the local environment.

463 Based on this evidence, a specifically designed correction factor could be
 464 introduced to take into account the non-negligible effect of the long-wave
 465 exchange, at least when horizontal applications are considered. In any case,
 466 the radiation-based forcing allowed to reproduce the thermal response of

the investigated waterproof-polyurethane-based roofing solutions in a rapid and effective way by exposing all the membranes to the same forcing cycle. The interaction between the short-wave incoming solar radiation and the different surfaces is, in this case, a real physical phenomenon that depends on the specific solar reflectance capability of the investigated membranes.

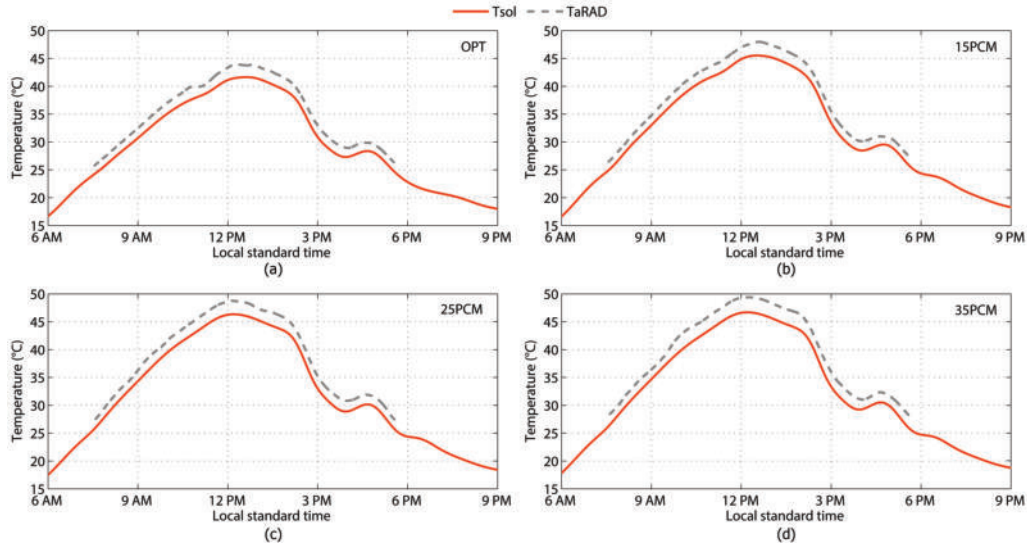


Figure 11: Comparison between the thermal profiles from the TaRAD and the Tsol cycle for the investigated polyurethane membranes, i.e. (a) OPT-CM, (b) 15PCM-CM, (c) 25PCM-CM, and (d) 35PCM-CM, before the accelerated weathering procedure.

5. Conclusions

Building upon previous research aimed at developing an innovative polyurethane membrane including up to 35%-in-weight of phase change materials with a melting temperature of 25 °C, this work tackles the thermo-optic durability of such unique application coupling cool and latent solutions into a composite roofing material for passive cooling purpose.

In more detail, the role of PCMs in improving the cool roof membrane durability when exposed to typical massive thermal fluctuations due to extreme air temperatures and intense radiation from the sun, was assessed.

By shifting from a purely sensible to a partly latent heat storage application, this research aimed to reduce the long-term deterioration of the

484 membrane due to extreme thermal stresses. In this view, three different roof
485 membranes including organic paraffin in a shape-stabilized solution were de-
486 veloped considering 15%, 25%, and 35% of PCM with respect to the weight of
487 the liquid membrane. Additionally, an optimized cool roof membrane includ-
488 ing titanium dioxide was also produced for comparison purpose. Said mem-
489 branes were later exposed to an accelerated weathering procedure (QUV) for
490 15, 30, and 60 days, according to ASTM D 4329-99 and ASTM G 154-06,
491 and their optic performance was evaluated in terms of reflection coefficient
492 based on ASTM E903-12 before and after the aging procedure. Finally, the
493 thermal performance of all the samples was investigated and compared in
494 terms of roof surface temperature using controlled environmental forcing. In
495 more detail, an ATT DM340SR climatic chamber equipped with a solar sim-
496 ulator (halogen lamp) was used to reproduce the local boundary conditions
497 of a typical summer day and expose the samples to a fully controlled and
498 reproducible environmental forcing. The behavior of the membranes was
499 compared using sol-air temperature-based forcing cycles, while the potential
500 use of radiation-based conditioning was assessed and bench-marked to the
501 previous methodology.

502
503 Results showed that the introduction of the latent additive allows to pre-
504 serve a more stable solar reflectance capability even after 60 days of ag-
505 ing, particularly when 25% in weight of PCM was added to the original
506 polyurethane-based mixture. Concerning the surface temperature monitor-
507 ing during controlled environmental forcing, PCM addition to the basic mix-
508 ture involved lower thermal performance at time zero, but in the meantime,
509 allowed to maintain a more stable behavior with increasing the weather-
510 ing time. In particular, the detrimental temperature increase registered be-
511 tween the new and the 15-days-aged OPT sample was significantly reduced
512 by the introduction of the PCM. Additionally, the 25% PCM solution not
513 only maintained its thermo-optic performance, but it actually improved, al-
514 though slightly, after 30 and 60 days of aging. As for the radiation-based
515 conditioning, it was shown that though this methodology tends to overstate
516 surface overheating due to the exclusion of the long-wave radiative exchange
517 with the sky, a specifically designed correction factor could be used to rapidly
518 produce reliable temperature profiles.

519
520 In conclusion, the proposed analysis showed how thermal energy storage
521 techniques could be used to improve the thermo-optic durability of water-

522 proof membranes for roofing applications, frequently exposed to severe degra-
523 dation due to extreme environmental boundary conditions. In particular, the
524 addition of the proper amount of latent storage material could produce a fin-
525 ishing material capable of improving rather than reducing its passive cooling
526 capability after extreme weathering conditions.

527 **Acknowledgment**

528 **Acknowledgment**

529 This research has received funding from the European Union’s Horizon
530 2020 research and innovation program under grant agreement n° 657466
531 (INPATH-TES). The authors would like to thank Fondazione cassa di Risparmio
532 di Perugia for supporting the investigation about bio-materials within the
533 project SOS CITTÁ 2018.0499.026 and Gabriele Franceschetti and CVR
534 s.r.l. company for assisting the development of cool membranes prototypes
535 with integrated PCMs. Cristina Pisellis acknowledgments are due to “Um-
536 bria A.R.CO.” project of Regione Umbria for supporting her research within
537 the framework of “SMEET-WELL: SMart building managEment for Energy
538 saving meets WELLbeing” project.

539 **References**

- 540 [1] L. Saikku, A. Rautiainen, P. E. Kauppi, The sustainability challenge of
541 meeting carbon dioxide targets in Europe by 2020, *Energy Policy* 36 (2)
542 (2008) 730–742. doi:10.1016/j.enpol.2007.10.007.
- 543 [2] N. Soares, J. Bastos, L. Dias Pereira, A. Soares, A. R. Amaral,
544 E. Asadi, F. Lamas, E. Rodrigues, H. Monteiro, M. Lopes, A. Gas-
545 par, A review on current advances in the energy and environmental
546 performance of buildings towards a more sustainable built environ-
547 ment, *Renewable and Sustainable Energy Reviews* 77 (2017) 845–860.
548 doi:10.1016/j.rser.2017.04.027.
- 549 [3] M. Walls, Energy efficiency: Building labels lead to savings, *Nature*
550 *Energy* 1 (2017) 17055. doi:10.1038/nenergy.2017.55.
- 551 [4] F. Ascione, Energy conservation and renewable technologies for build-
552 ings to face the impact of the climate change and minimize the use of
553 cooling, *Solar Energy* 154. doi:10.1016/j.solener.2017.01.022.

- 554 [5] D. Jacob, L. Kotova, C. Teichmann, S. Sobolowski, R. Vautard, C. Don-
 555 nelly, A. Koutroulis, M. Grillakis, I. Tsanis, A. Damm, A. Sakalli, M. van
 556 Vliet, Climate impacts in Europe under +1.5°C global warming, *Earth's*
 557 *Future* doi:10.1002/2017EF000710.
- 558 [6] M. Santamouris, Cooling the buildings past, present and future, *Energy*
 559 *and Buildings* 128. doi:10.1016/j.enbuild.2016.07.034.
- 560 [7] M. Kaboré, E. Bozonnet, P. Salagnac, M. Abadie, Indexes
 561 for passive building design in urban context—indoor and out-
 562 door cooling potentials, *Energy and Buildings* 173 (2018) 315–325.
 563 doi:10.1016/j.enbuild.2018.05.043.
- 564 [8] H. Akbari, H. D. Matthews, Global cooling updates: Reflec-
 565 tive roofs and pavements, *Energy and Buildings* 55 (2012) 26.
 566 doi:10.1016/j.enbuild.2012.02.055.
- 567 [9] H. Akbari, C. Cartalis, D. Kolokotsa, A. Muscio, A. L. Pisello,
 568 F. Rossi, M. Santamouris, A. Synnefa, N. Wong, M. Zinzi, Local cli-
 569 mate change and urban heat island mitigation techniques - the state of
 570 the art, *Journal of Civil Engineering and Management* 22 (2016) 1–16.
 571 doi:10.3846/13923730.2015.1111934.
- 572 [10] P. Rosado, R. Levinson, Potential benefits of cool walls on resi-
 573 dential and commercial buildings across california and the united
 574 states: Conserving energy, saving money, and reducing emission
 575 of greenhouse gases and air pollutants, *Energy and Buildings* 199.
 576 doi:10.1016/j.enbuild.2019.02.028.
- 577 [11] T. Xu, J. Sathaye, H. Akbari, V. Garg, S. Tetali, Quantifying the direct
 578 benefits of cool roofs in an urban setting: Reduced cooling energy use
 579 and lowered greenhouse gas emissions, *Building and Environment* 48
 580 (2012) 1–6. doi:10.1016/j.buildenv.2011.08.011.
- 581 [12] A. H. Rosenfeld, H. Akbari, J. J. Romm, M. Pomerantz, Cool commu-
 582 nities: strategies for heat island mitigation and smog reduction, *Energy*
 583 *and buildings* 28 (1) (1998) 51–62. doi:10.1016/S0378-7788(97)00063-7.
- 584 [13] M. Pomerantz, Are cooler surfaces a cost-effect mitigation of
 585 urban heat islands?, *Urban Climate* 24 (2018) 393 – 397.
 586 doi:10.1016/j.uclim.2017.04.009.

- [14] C. Piselli, M. Saffari, A. de Gracia, A. L. Pisello, F. Cotana, L. F. Cabeza, Optimization of roof solar reflectance under different climate conditions, occupancy, building configuration and energy systems, *Energy and Buildings* 151 (2017) 81–97. doi:10.1016/j.enbuild.2017.06.045.
- [15] I. Hernández-Pérez, J. Xamán, E. V. Macías-Melo, K. M. Aguilar-Castro, I. Zavala-Guillén, I. Hernández-López, E. Simá, Experimental thermal evaluation of building roofs with conventional and reflective coatings, *Energy and Buildings* 158 (2018) 569–579. doi:10.1016/j.enbuild.2017.09.085.
- [16] P. Meenakshi, M. Selvaraj, Bismuth titanate as an infrared reflective pigment for cool roof coating, *Solar Energy Materials and Solar Cells* 174 (2018) 530–537. doi:10.1016/j.solmat.2017.09.048.
- [17] A. de Gracia, L. F. Cabeza, Phase change materials and thermal energy storage for buildings, *Energy and Buildings* 88. doi:10.1016/j.enbuild.2015.06.007.
- [18] M. Song, F. Niu, N. Mao, Y. Hu, S. Deng, Review on building energy performance improvement using phase change materials, *Energy and Buildings* 158 (2018) 776–793. doi:10.1016/j.enbuild.2017.10.066.
- [19] K. Kant, A. Shukla, A. Sharma, Advancement in phase change materials for thermal energy storage applications, *Solar Energy Materials and Solar Cells* 172 (2017) 82–92. doi:10.1016/j.solmat.2017.07.023.
- [20] L. Calabrese, E. Proverbio, A. Frazzica, V. Brancato, F. Grungo, D. La Rosa, V. Palomba, Thermal performance of hybrid cement mortar-PCMs for warm climates application, *Solar Energy Materials and Solar Cells* 193 (2019) 270–280. doi:10.1016/j.solmat.2019.01.022.
- [21] H. B. Kim, M. Mae, Y. Choi, T. Kiyota, Experimental analysis of thermal performance in buildings with shape-stabilized phase change materials, *Energy and Buildings* 152 (2017) 524–533. doi:10.1016/j.enbuild.2017.07.076.
- [22] M. Genc, Z. Genc, Microencapsulated myristic acid/fly ash with tio₂ shell as a novel phase change material for building application, *Journal of Thermal Analysis and Calorimetry* 131 (2017) 1–8. doi:10.1007/s10973-017-6781-7.

- [23] I. Krupa, P. Sobolčiak, H. Abdelrazeq, M. Ouederni, M. A. Al-Maadeed, Natural aging of shape stabilized phase change materials based on paraffin wax, *Polymer testing* 63 (2017) 567–572. doi:10.1016/j.polymertesting.2017.09.027.
- [24] Z. Rao, G. Zhang, T. Xu, K. Hong, Experimental study on a novel form-stable phase change materials based on diatomite for solar energy storage, *Solar Energy Materials and Solar Cells* 182 (2018) 52–60. doi:10.1016/j.solmat.2018.03.016.
- [25] S. G. Yoon, Y. K. Yang, T. W. Kim, M. H. Chung, J. C. Park, Thermal performance test of a phase-change-material cool roof system by a scaled model, *Advances in Civil Engineering* 2018. doi:10.1155/2018/2646103.
- [26] A. Pisello, E. Fortunati, S. Mattioli, L. F. Cabeza, C. Barreneche, J. Kenny, F. Cotana, Innovative cool roofing membrane with integrated phase change materials: Experimental characterization of morphological, thermal and optic-energy behavior, *Energy and Buildings* 112 (2016) 40–48. doi:10.1016/j.enbuild.2015.11.061.
- [27] P. Lassandro, S. Di Turi, Energy efficiency and resilience against increasing temperatures in summer: The use of pcm and cool materials in buildings, *International Journal of Heat and Technology* 35 (2017) S307–S315. doi:10.18280/ijht.35Sp0142.
- [28] Y. K. Yang, I. S. Kang, M. H. Chung, S. Kim, J. C. Park, Effect of pcm cool roof system on the reduction in urban heat island phenomenon, *Building and Environment* 122 (2017) 411 – 421. doi:10.1016/j.buildenv.2017.06.015.
- [29] S. Lu, Y. Chen, S. Liu, X. Kong, Experimental research on a novel energy efficiency roof coupled with pcm and cool materials, *Energy and Buildings* 127. doi:10.1016/j.enbuild.2016.05.080.
- [30] M. Saffari, C. Piselli, A. de Gracia, A. L. Pisello, F. Cotana, L. F. Cabeza, Thermal stress reduction in cool roof membranes using phase change materials (pcm), *Energy and Buildings* 158 (2018) 1097–1105. doi:10.1016/j.enbuild.2017.10.068.

- [31] S. Tsoka, T. Theodosiou, K. Tsikaloudaki, F. Flourentzou, Modeling the performance of cool pavements and the effect of their aging on outdoor surface and air temperatures, *Sustainable Cities and Society* 42. doi:10.1016/j.scs.2018.07.016.
- [32] M. Sleiman, G. Ban-Weiss, H. E. Gilbert, D. François, P. Berdahl, T. W. Kirchstetter, H. Destailats, R. Levinson, Soiling of building envelope surfaces and its effect on solar reflectance part i: Analysis of roofing product databases, *Solar Energy Materials and Solar Cells* 95 (12) (2011) 3385–3399. doi:10.1016/j.solmat.2011.08.002.
- [33] M. Sleiman, T. W. Kirchstetter, P. Berdahl, H. E. Gilbert, S. Quelen, L. Marlot, C. V. Preble, S. Chen, A. Montalbano, O. Rosseler, et al., Soiling of building envelope surfaces and its effect on solar reflectance—part ii: Development of an accelerated aging method for roofing materials, *Solar Energy Materials and Solar Cells* 122 (2014) 271–281. doi:10.1016/j.solmat.2013.11.028.
- [34] M. Sleiman, S. Chen, H. E. Gilbert, T. W. Kirchstetter, P. Berdahl, E. Bibian, L. S. Bruckman, D. Cremona, R. H. French, D. A. Gordon, et al., Soiling of building envelope surfaces and its effect on solar reflectance—part iii: Interlaboratory study of an accelerated aging method for roofing materials, *Solar Energy Materials and Solar Cells* 143 (2015) 581–590. doi:10.1016/j.solmat.2011.08.002.
- [35] C. Ferrari, G. Santunione, A. Libbra, A. Muscio, E. Sgarbi, How accelerated biological aging can affect solar reflective polymeric based building materials, *Journal of Physics: Conference Series* 923 (2017) 012046. doi:10.1088/1742-6596/923/1/012046.
- [36] R. Levinson, P. Berdahl, A. Berhe, H. Akbari, Effect of soiling and cleaning on reflectance and solar heat gain of a light-colored roofing membrane, *Atmospheric Environment* 39 (2005) 7807–7824. doi:10.1016/j.atmosenv.2005.08.037.
- [37] M. LLC, Cool Roof Rating Council, <https://coolroofs.org/>, accessed: 2019-10-24.
- [38] N. Alchapar, E. Correa, Aging of roof coatings. solar reflectance stability according to their morphological characteris-

- 684 tics, *Construction and Building Materials* 102 (2016) 297–305.
685 doi:10.1016/j.conbuildmat.2015.11.005.
- 686 [39] E. Mastrapostoli, M. Santamouris, D. Kolokotsa, P. Vassilis, D. Ve-
687 nieri, K. Gompakis, On the ageing of cool roofs: Measure of the
688 optical degradation, chemical and biological analysis and assessment
689 of the energy impact, *Energy and Buildings* 114 (2016) 191 – 199.
690 doi:doi.org/10.1016/j.enbuild.2015.05.030.
- 691 [40] C. Ferrari, A. Gholizadeh Touchaei, M. Sleiman, A. Libbra, A. Muscio,
692 C. Siligardi, H. Akbari, Effect of aging processes on solar reflectivity
693 of clay roof tiles, *Advances in Building Energy Research* 8 (1) (2014)
694 28–40. doi:10.1080/17512549.2014.890535.
- 695 [41] R. F. De Masi, S. Ruggiero, G. P. Vanoli, Acrylic white paint of in-
696 dustrial sector for cool roofing application: Experimental investigation
697 of summer behavior and aging problem under Mediterranean climate,
698 *Solar Energy* 169 (2018) 468–487. doi:10.1016/j.solener.2018.05.021.
- 699 [42] T. Aoyama, T. Sonoda, Y. Nakanishi, J. Tanabe, H. Take-
700 bayashi, Study on aging of solar reflectance of the self-cleaning
701 high reflectance coating, *Energy and Buildings* 157 (2017) 92–100.
702 doi:10.1016/j.enbuild.2017.02.021.
- 703 [43] X. Yang, C. Vang, D. Tallman, G. Bierwagen, S. Croll, S. Rohlik, Weath-
704 ering degradation of polyurethane coating, *Polymer Degradation and*
705 *Stability* 74 (2001) 341–351. doi:10.1016/S0141-3910(01)00166-5.
- 706 [44] B. Jelle, Accelerated climate ageing of building materials, components
707 and structures in the laboratory, *Journal of Materials Science* 47 (2012)
708 6475–6496. doi:10.1007/s10853-012-6349-7.
- 709 [45] A. L. Pisello, E. Fortunati, C. Fabiani, S. Mattioli, F. Dominici, L. Torre,
710 L. F. Cabeza, F. Cotana, Pcm for improving polyurethane-based cool
711 roof membranes durability, *Solar Energy Materials and Solar Cells* 160
712 (2017) 34 – 42. doi:10.1016/j.solmat.2016.09.036.
- 713 [46] G. Santunione, C. Ferrari, C. Siligardi, A. Muscio, E. Sgarbi, Accel-
714 erated biological ageing of solar reflective and aesthetically relevant
715 building materials, *Advances in Building Energy Research* (2018) 1–
716 18doi:10.1080/17512549.2018.1488616.

- [47] R. Ye, W. Lin, K. Yuan, X. Fang, Z. Zhang, Experimental and numerical investigations on the thermal performance of building plane containing $\text{CaCl}_2 \cdot 6\text{H}_2\text{O}$ /expanded graphite composite phase change material, *Applied Energy* 193 (2017) 325–335. doi:10.1016/j.apenergy.2017.02.049.
- [48] C. Piselli, V. Castaldo, A. L. Pisello, How to enhance thermal energy storage effect of pcm in roofs with varying solar reflectance: Experimental and numerical assessment of a new roof system for passive cooling in different climate conditions, *Solar Energy* doi:10.1016/j.solener.2018.06.047.
- [49] R. Ricci, L. A. Besalduch, A. Galatioto, G. Ciulla, Thermal characterization of insulating materials, *Renewable and Sustainable Energy Reviews* 82 (2016) 1765–1773. doi:10.1016/j.rser.2017.06.057.
- [50] A. D'Alessandro, A. L. Pisello, C. Fabiani, F. Ubertini, L. F. Cabeza, F. Cotana, Multifunctional smart concretes with novel phase change materials: Mechanical and thermo-energy investigation, *Applied Energy* 212 (2018) 1448–1461. doi:10.1016/j.apenergy.2018.01.014.
- [51] M. H. Chung, J. C. Park, Development of PCM cool roof system to control urban heat island considering temperate climatic conditions, *Energy and Buildings* 116 (2016) 341–348. doi:10.1016/j.enbuild.2015.12.056.
- [52] A. L. Pisello, V. Castaldo, G. Pignatta, M. Santamouris, F. Cotana, Experimental in-lab and in-field analysis of waterproof membranes for cool roof application and urban heat island mitigation, *Energy and Buildings* 114 (2016) 180–190. doi:10.1016/j.enbuild.2015.05.026.
- [53] ASTM D4329-13, Standard practice for fluorescent ultraviolet (uv) lamp apparatus exposure of plastics, Standard, ASTM International, West Conshohocken, PA (2013). doi:10.1520/D4329-13.
- [54] ASTM G154-06, Standard Practice for Operating Fluorescent Light Apparatus for UV Exposure of Nonmetallic Materials, Standard, ASTM International, West Conshohocken, PA (2006). doi:10.1520/G0154-12A.
- [55] ASTM E903-12, Standard Test Method for Solar Absorptance, Reflectance, and Transmittance of Materials Using Integrating Spheres, Standard, ASTM International, West Conshohocken, PA (2012). doi:10.1520/E0903-12.

- 750 [56] Angelantoni Test Technologies, http://www.acstestchambers.com/Product/Prodotto?id_fam=
751 (2012).
- 752 [57] ASTM G173-03(2012), Standard tables for reference solar spectral
753 irradiances: Direct normal and hemispherical on 37° tilted sur-
754 face, Standard, ASTM International, West Conshohocken, PA (2012).
755 doi:10.1520/G0173-03R12.
- 756 [58] A. V. Sá, M. Azenha, H. De Sousa, A. Samagaio, Thermal enhance-
757 ment of plastering mortars with phase change materials: Experimen-
758 tal and numerical approach, *Energy and Buildings* 49 (2012) 1627.
759 doi:10.1016/j.enbuild.2012.02.031.
- 760 [59] ISO 6946:2017, Building components and building elements – Thermal
761 resistance and thermal transmittance – Calculation methods, Standard,
762 International Organization for Standardization, Geneva, CH (2017).
763 URL <https://www.iso.org/standard/40968.html>
- 764 [60] J. F. Kreider, P. S. Curtiss, A. Rabl, Heating and cooling of buildings:
765 design for efficiency, edition, r Edition, Vol. 32, Taylor & Francis Group,
766 2013. doi:10.5860/choice.32-1554.
- 767 [61] V. Castaldo, V. Coccia, F. Cotana, G. Pignatta, A. L. Pisello, F. Rossi,
768 Thermal-energy analysis of natural “cool” stone aggregates as passive
769 cooling and global warming mitigation technique, *Urban Climate* 14.
770 doi:10.1016/j.uclim.2015.05.006.